2021 IEEE International Conference on Robotics and Automation (ICRA 2021)
May 31 - June 4, 2021, Xi'an, China

Positioning Control for Underactuated Unmanned Surface Vehicles to Resist Environmental Disturbances

Yang Qu and Lilong Cai

Abstract— **In this paper, we present the positioning control problem for underactuated unmanned surface vehicles (USVs) in the presence of unknown external disturbances, such as the wind, waves, and currents. The three control objectives of positioning control for underactuated USVs are, firstly, to retain a predefined constant distance to a look-ahead point, secondly, to regulate the vehicle heading to point at the look-ahead point and, thirdly, to update the position of the look-ahead point to rotate the USVs. Particularly, a new guidance rule is proposed to update the look-ahead point based on the positioning error such that the predefined desired position is maintained and the vehicle heading is counter to the direction of resultant environmental force at the same time. To illustrate the stability of the positioning control system, the error dynamics driven by the component of resultant environmental force is derived and analyzed. In addition to the simulations, experiments were carried out offshore in the face of wind and waves to verify the validity and effectiveness of the proposed method.**

I. Introduction

With the development of marine technology and rising labor costs, the social and economic development has become more and more dependent on the application of unmanned surface vehicles (USVs) to carry out dangerous and routine activities in hazardous areas and extreme working conditions, such as resource exploration, construction of seabed pipes, maritime rescue and firefighting, and offshore surveillance [1]–[4]. Particularly, the accomplishment of some tasks requires the USVs to have the ability to keep its position for a long period of time. For fully actuated marine surface vehicles with multiple actuators, position keeping is well researched and has been put into real implementation for commercial ships and oil drilling platforms, i.e. dynamic positioning system [5]–[8]. Most USVs, however, are typically underactuated [9], and one main propeller and a rudder, two main propellers, or one azimuth thruster may be the configuration. Hence, there is no direct control input to satisfy the control objective in lateral direction (sway control), which makes it difficult to retain the position of the vehicle especially in the presence of external disturbances, i.e. wind, waves, and currents.

If both the desired position and orientation are specified for underactuated USVs, the orientation of vehicle should be regularly modified by the yaw moment input along with the surge control input to produce a force to control the sway variables [10]–[14]. This kind of frequent adaptation consumes more energy and can induce wear and tear of the actuators. Particularly, [15] provided a positioning control method for surface marine vehicles with only the desired position defined, and the desired heading was adaptively adjusted based on the deviation of position until the vehicle's heading was counter to the direction of resultant environmental forces. By imitating the pendulum motion in gravity, the implementation of the nonlinear model based backstopping approach in [15] was derived in four steps and involves an accurate mathematical model. To obtain the model parameters, model identification is typically conducted for fully actuated marine vehicles [4], [16], [17]. Hence, the implementation of model based control system design for underactuated USVs is limited due to the lack of model parameters.

A vehicle-independent positioning control strategy will be introduced in this paper in order to enforce this control algorithm for underactuated USVs. The aim of surge control is to maintain a consistent distance between the vehicle and a look-ahead point. The yaw objective is to make the vehicle's heading track the desired orientation that points to the look-ahead point. Considering that the angle deviation between the vehicle's heading and the direction of resultant environmental forces would create a vehicle's lateral drift movement, the look-ahead point that travels around the target location with the predefined constant circle radius must also be modified and updated to minimize the position deviation. The control technique to change the look-ahead point at the predefined circle around the target location will be emphasized and built in this paper. In order to verify the proposed positioning control system for underactuated USVs, both simulations and experiments have been carried out.

This paper is structured as follows. Section II presents the mathematical modeling of USVs, and the problem formulation in polar coordinates. Section III describes the control algorithms design in surge and yaw directions, and the adaptive rule of desired yaw heading to minimize the deviation of position. The design and system implementation of the USV prototype in experiment is described in Section IV. Simulations, experimental results, and discussions are presented in Section V. Section VI ends this paper.

II. Problem Formulation

For marine surface vehicles, the three degree-of-freedom (DOF) mathematical model is established in the North-East coordinates and Body-Fixed coordinates, shown in Fig. 1. According to [8], it can be expressed as

$$\dot{\boldsymbol{\eta}} = \boldsymbol{J}(\psi)\boldsymbol{v} \tag{1}$$

Y. Qu, and L. Cai are with the Department of Mechanical and Aerospace Engineering, School of Engineering, The Hong Kong University of Science and Technology, Hong Kong SAR, China. yquae@connect.ust.hk, melcai@ust.hk

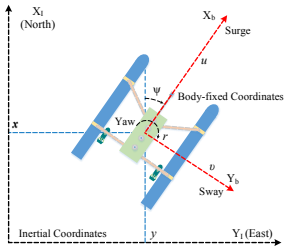

Fig. 1. The definition of USV coordinates.

$$\boldsymbol{M}\dot{\boldsymbol{v}} + \boldsymbol{C}(\boldsymbol{v})\boldsymbol{v} + \boldsymbol{D}(\boldsymbol{v})\boldsymbol{v} = \boldsymbol{B}\boldsymbol{\tau} + \boldsymbol{\tau}_e \tag{2}$$

where vector $\boldsymbol{\eta} = [x, y, \psi]^{\mathrm{T}}$ contains the position and orientation in inertial coordinates, $\boldsymbol{v} = [u, \nu, r]^{\mathrm{T}}$ denotes the velocity vector in the surge, sway, and yaw directions, $\boldsymbol{J}(\psi) \in \Re^{3\times 3}$ is the rotational matrix converting the states between the inertial and body-fixed coordinates and described as

$$\boldsymbol{J}(\psi) = \begin{bmatrix} \cos\psi & -\sin\psi & 0 \\ \sin\psi & \cos\psi & 0 \\ 0 & 0 & 1 \end{bmatrix},$$

$\boldsymbol{M}$ is the mass matrix with the added mass and the inertial mass, $\boldsymbol{C}(\boldsymbol{v})$ is the Coriolis and centripetal matrix, $\boldsymbol{D}(\boldsymbol{v})$ is the hydrodynamic damping matrix including the skin friction, potential damping carried in generated waves, and vortex shedding, $\boldsymbol{\tau_e} \in \Re^{3\times 1}$ is the environmental forces including wind, waves, and currents, $\boldsymbol{B}$ is the configuration matrix of actuators, and $\boldsymbol{\tau}$ is the control input forces and moment generated by actuators. The detailed formulations of these matrices are given in [8], [17]. Since the proposed positioning control method in this paper is vehicle-independent, the model parameters in (2) are only used in the simulations instead of the real positioning control implementation.

Particularly, the underactuated USVs usually have the actuators to generate the surge force and yaw moment which yields

$$\boldsymbol{B} = \begin{bmatrix} 1 & 0 \\ 0 & \kappa \\ 0 & 1 \end{bmatrix}, \quad \boldsymbol{\tau} = \begin{bmatrix} \tau_{surge} \\ \tau_{yaw} \end{bmatrix}.$$

where κ is the parameter related to the yaw control determined by the actuator configuration. It needs to be emphasized that the problem of positioning control for underactuated USVs is to derive the control algorithm to update the desired orientation of USVs such that the environmental force in sway direction can act as the third control input to minimize the positioning deviation. The sway dynamics driven by the environmental force is derived and analyzed in the Subsection D.

A. Restricted Circle Motion and Control Objectives

Taking into account the restricted motion in the working area with disturbances, the USV always regulates its heading to point at a look-ahead point (x_o, y_o) and concurrently maintains a predefined distance to this look-ahead point, shown as Fig. 2. Similar to the pendulum motion in gravity,

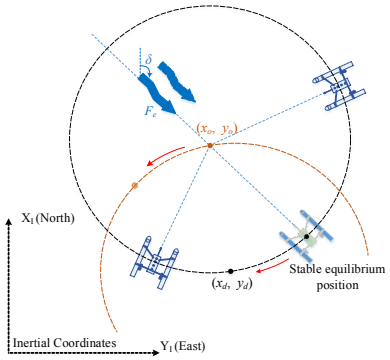

Fig. 2. Stable equilibrium position in the restricted circle movement.

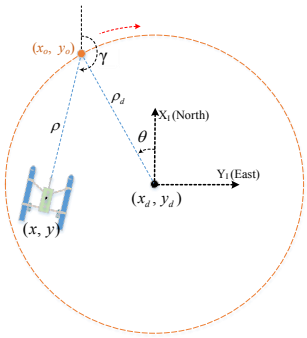

Fig. 3. To update look-ahead point in polar coordinates.

the unique stable equilibrium position is maintained when the vehicle's heading was counter to the direction of resultant environmental forces. It is worth pointing out that the selection of look-ahead point (x_o, y_o) has a direct effect on the stable equilibrium position. If the look-ahead point (x_o, y_o) moves around the target location (x_d, y_d) with the predefined constant circle radius, therefore, it is conceivable that there exists appropriate way to update the look-ahead point (x_o, y_o) such that the desired position can be reached and maintained at the stable equilibrium position.

Hereby, the corresponding control objectives are:

1) *Surge Control*: To maintain the constant distance to the look-ahead point (x_o, y_o), i.e. $\rho = \rho_d$.
2) *Yaw Control*: To force the heading of vehicle to point at the look-ahead point (x_o, y_o), i.e. $\psi = \gamma + \pi$.
3) *The update of the look-ahead point*: To derive the update law for the look-ahead point (x_o, y_o) to minimize the position deviation, i.e. the update of θ.

B. USV Kinematics in Polar Coordinates

To illustrate the positioning control problem for USVs, it is necessary to introduce the polar coordinates, shown in Fig. 3. The USV position (x, y) can be denoted as

$$x = x_o + \rho\cos\gamma \tag{3}$$

$$y = y_o + \rho\sin\gamma \tag{4}$$

where (x_o, y_o) is the look-ahead point, ρ is the distance between vehicle and (x_o, y_o), and γ is the azimuth angle.

It follows that

$$\rho = \sqrt{(x - x_o)^2 + (y - y_o)^2} \tag{5}$$

$$\gamma = \arctan2\left(y - y_o,\ x - x_o\right) \tag{6}$$

As shown in Fig. (3), define the constant radius ρ_d, and we have

$$x_o = x_d + \rho_d \cos\theta \tag{7}$$

$$y_o = y_d + \rho_d \sin\theta \tag{8}$$

By inserting (7) and (8) into (3) and (4) respectively, the first order derivatives of (3) and (4) with respect to time gives

$$\dot{x} = -\dot{\theta}\rho_d \sin\theta + \dot{\rho}\cos\gamma - \rho\dot{\gamma}\sin\gamma \tag{9}$$

$$\dot{y} = \dot{\theta}\rho_d \cos\theta + \dot{\rho}\sin\gamma + \rho\dot{\gamma}\cos\gamma \tag{10}$$

Define the vectors $\boldsymbol{L} = [-\dot{\theta}\rho_d \sin\theta,\ \dot{\theta}\rho_d \cos\theta,\ 0]^{\mathrm{T}}$ and $\boldsymbol{X} = [\rho,\ \gamma,\ \psi]^{\mathrm{T}}$. Rewrite (9) and (10) as the following matrix form

$$\dot{\boldsymbol{\eta}} = \boldsymbol{J}(\gamma)\boldsymbol{H}(\rho)\dot{\boldsymbol{X}} + \boldsymbol{L} \tag{11}$$

where

$$\boldsymbol{J}(\gamma) = \begin{bmatrix} \cos(\gamma) & -\sin(\gamma) & 0 \\ \sin(\gamma) & \cos(\gamma) & 0 \\ 0 & 0 & 1 \end{bmatrix}, \boldsymbol{H}(\rho) = \begin{bmatrix} 1 & 0 & 0 \\ 0 & \rho & 0 \\ 0 & 0 & 1 \end{bmatrix}.$$

The kinematics in polar coordinates can be formulated by combining (1) and (11), given by

$$\dot{\boldsymbol{X}} = \boldsymbol{H}^{-1}(\rho)\boldsymbol{J}(\psi - \gamma)\boldsymbol{v} - \boldsymbol{H}^{-1}(\rho)\boldsymbol{J}^{\mathrm{T}}(\gamma)\boldsymbol{L} \tag{12}$$

C. Cascaded System Stability

The USV has adequate control authority to achieve independent surge and yaw control ability to make the corresponding dynamics globally stable

$$\Sigma_1 : \begin{cases} M_{11}\ddot{\tilde{\rho}} + N_{\tilde{\rho}} = -\tau_{surge}\cos\tilde{\psi} \\ M_{33}\ddot{\tilde{\psi}} + N_{\tilde{\psi}} = \tau_{yaw} \end{cases} \tag{13}$$

where M_{11} is surge mass, M_{33} is yaw inertial moment, $\tilde{\rho} = \rho - \rho_d$, $\tilde{\psi} = \psi - \psi_d$, $N_{\tilde{\rho}}$ and $N_{\tilde{\psi}}$ contain the nonlinear terms and environmental forces accordingly.

The lateral movement of the USV is what we are concerned about in positioning control scenario. By expending (12), the second subsystem with sway dynamics give

$$\Sigma_2 : \begin{cases} \rho_d\dot{\gamma} = -\nu - \rho_d\cos(\theta - \gamma)\dot{\theta} + f \\ M_{22}\dot{\nu} + N_\nu = \tau_e(2) + \kappa\tau_{yaw} \end{cases} \tag{14}$$

where M_{22} is the mass in sway, N_ν is the nonlinear term, $\tau_e(2)$ is the sway environmental from the bow, $f = -\dot{\gamma}\tilde{\rho} - u\sin\tilde{\psi} + \nu(1 - \cos\tilde{\psi})$, and $|f| \le |\dot{\gamma}||\tilde{\rho}| + (|u| + |\nu\tilde{\psi}/2|)|\tilde{\psi}| \le K_1|\tilde{\rho}| + K_2|\tilde{\psi}|$. Since yaw moment is usually generated by actuators from stern, we have $|\kappa\tau_{yaw} - \zeta\tau_e(2)| \le K_3|\tilde{\psi}|$ and $0 < \zeta < 1$. Without loss of generality, the yaw effect can be ignored by $\zeta = 0$. Since subsystem Σ_1 is stable, the stability of cascaded system Σ_1 and Σ_2 is equivalent to analyze the stability of Σ_2 with $f = 0$ and $\kappa\tau_{yaw} = 0$ [18], [19], which is discussed in the rest of paper.

D. USV Sway Dynamics in Polar Coordinates

Through the analysis above, (14) with $f = 0$ yields

$$\nu = -\rho_d\dot{\gamma} - \rho_d\cos(\theta - \gamma)\dot{\theta} \tag{15}$$

$$\dot{\nu} = -\rho_d\ddot{\gamma} - \rho_d\cos(\theta - \gamma)\ddot{\theta} + \rho_d(\dot{\theta} - \dot{\gamma})\sin(\theta - \gamma)\dot{\theta} \tag{16}$$

Let $\boldsymbol{N} = \boldsymbol{C}(\boldsymbol{v}) + \boldsymbol{D}(\boldsymbol{v})$ denote the nonlinear terms of USV dynamics (2). Since the surge and sway dynamics are uncoupled from each other, the second row of the matrix $\boldsymbol{N}$ and mass matrix $\boldsymbol{M}$ can be written $[0,\ N_{22},\ N_{23}]$ and $[0,\ M_{22},\ M_{23}]$ respectively [8]. Inserting (15) and (16) into the sway dynamics of (2) gives the following dynamics of γ in polar coordinates.

$$\begin{aligned} &M_{22}\rho_d\left[-\ddot{\gamma} - \cos(\theta - \gamma)\ddot{\theta} + (\dot{\theta} - \dot{\gamma})\sin(\theta - \gamma)\dot{\theta}\right] + M_{23}\dot{r} \\ &+N_{22}\rho_d\left[-\dot{\gamma} - \cos(\theta - \gamma)\dot{\theta}\right] + N_{23}r = \tau_e(2) \end{aligned} \tag{17}$$

As shown in Fig. 2, let F_e represent the magnitude of resultant environmental force and δ denote its direction in the inertial coordinates. In body-fixed coordinates, the sway component of the environmental force can be written as

$$\begin{aligned} \tau_e(2) &= -\sin(\psi)F_e\cos(\delta) + \cos(\psi)F_e\sin(\delta) \\ &= F_e\sin(\delta - \psi) \end{aligned} \tag{18}$$

Considering that $r \approx \dot{\gamma}$ and $\dot{r} \approx \ddot{\gamma}$, the dynamics (17) driven by the environmental force can be rewritten as

$$\begin{aligned} &M_{22}\rho_d\left[-\ddot{\gamma} - \cos(\theta - \gamma)\ddot{\theta} + (\dot{\theta} - \dot{\gamma})\sin(\theta - \gamma)\dot{\theta}\right] + M_{23}\ddot{\gamma} \\ &+N_{22}\rho_d\left[-\dot{\gamma} - \cos(\theta - \gamma)\dot{\theta}\right] + N_{23}\dot{\gamma} = F_e\sin(\delta - \gamma - \pi) \end{aligned} \tag{19}$$

Remark 1: Equation (19) demonstrates the dynamics in the rotated direction around the look-ahead point (x_o, y_o) when the desired orientation $\gamma + \pi$ and the predefined distance ρ_d are maintained. For a constant look-ahead point (x_o, y_o), i.e. $\dot{\theta} = 0$ and $\ddot{\theta} = 0$, the stable equilibrium heading $\psi = \gamma + \pi = \delta$ will be obtained, which has been illustrated in Fig. 2. However, this stable equilibrium position may not be coincident with the predefined desired position, which is the reason why the look-ahead point (x_o, y_o) should be updated to adjust the stable equilibrium position at the same time.

III. Control System Design

A. Surge Control

To maintain the constant distance ρ_d to the look-ahead point, the tracking error in surge direction can be formulated as

$$e_\rho = \cos(\psi - \gamma - \pi)(\rho - \rho_d) \tag{20}$$

Hence, a classical PID control can be designed in surge direction

$$\tau_{surge} = -K_p e_\rho - K_i\int_0^t e_\rho dt - K_d\dot{e}_\rho \tag{21}$$

where K_p, K_i, and K_d are positive definite parameters.

B. Yaw Control

To track the desired orientation $\psi_d = \gamma + \pi$, define the following tracking error of orientation

$$e_\psi = \psi - \gamma - \pi \tag{22}$$

The classical PI control in yaw direction is formulated as

$$\tau_{yaw} = -\lambda_p e_\psi - \lambda_i \int_0^t e_\psi dt \tag{23}$$

where λ_p and λ_i are positive definite parameters.

C. Update Law for The Look-ahead Point

Define the following angle deviation

$$e = \theta - (\gamma + \pi) \tag{24}$$

To minimize the deviation of position, the updated law for the look-ahead point (x_o, y_o) is proposed as

$$\dot{\theta} = -ke, \qquad \sigma > k > 0 \tag{25}$$

where σ is the maximum value of k and will be determined below.

$Proposition1$: With the updated law (25), the angle deviation e will converge to zero driven by the sway component of resultant environmental force.

$Proof$: Using the updated law (25), the first and second order derivatives of (24) with respect to time gives

$$\dot{\gamma} = -ke - \dot{e} \tag{26}$$

$$\ddot{\gamma} = -k\dot{e} - \ddot{e} \tag{27}$$

Inserting (24)-(27) into the dynamics (19) yields

$$M_e\ddot{e} + N_e\dot{e} + K_e e = F_e \sin(\delta + e - \theta) \tag{28}$$

where the three coefficients are given by

$$M_e = M_{22}\rho_d - M_{23},$$

$$N_e = kM_{22}\rho_d(1 + e\sin e - \cos e) - kM_{23} + N_{22}\rho_d - N_{23},$$

$$K_e = kN_{22}\rho_d(1 - \cos e) - kN_{23},$$

and N_e and K_e are slowly varying.

For marine surface vessels, the mass matrix $\boldsymbol{M}$ and nonlinear matrix $\boldsymbol{N}$ are usually diagonal dominant matrices, therefore, $M_{22} > M_{23}$ and $N_{22} > N_{23}$ [6]. In the positioning control scenario, the predefined distance can be set as $\rho_d > 1$ to yield $M_e > 0$. Further, there exists a small positive value σ for $0 < k < \sigma$ to derive $N_e > 0$.

Let $\hat{\delta}$ denote the estimation of δ, and $\tilde{\delta} = \delta - \hat{\delta}$ denote the estimation error. Give the estimation $\hat{\delta}$ as follows

$$\hat{\delta} = \theta + \pi \tag{29}$$

Considering that δ is slowly varying, i.e. $\dot{\tilde{\delta}} = -\dot{\hat{\delta}}$, we have

$$\dot{\tilde{\delta}} = -\dot{\theta} = ke \tag{30}$$

Inserting $\tilde{\delta} = \delta - \hat{\delta}$, (29), and (30) into dynamics (28), it follows that

$$M_e\ddot{e} + N_e\dot{e} + K_e e = -F_e \sin(k\int_0^t edt + e) \tag{31}$$

Globally BIBO Stability of (31): Since the coefficient K_e and external input $F_e \sin(k\int_0^t edt + e)$ are well bounded, therefore, the output e is globally bounded [20].

Theorem 1: For nonlinear autonomous system $\dot{\boldsymbol{x}} = g(\boldsymbol{x})$, $g(0) = 0$, suppose that $g(\boldsymbol{x})$ is continuously differentiable and define $A = \partial g/\partial \boldsymbol{x}|_{\boldsymbol{x}=0}$. Then, $\boldsymbol{x} = 0$ is an exponentially stable equilibrium of nonlinear system $\dot{\boldsymbol{x}} = g(\boldsymbol{x})$ if and only if the linear state matrix A is Hurwitz [20].

Locally Exponentially Stability of (31): Define $\boldsymbol{x} = [\int_0^t edt,\ e,\ \dot{e}]^{\mathrm{T}}$, and Theorem 1 can be used to linearize (31) as $\dot{\boldsymbol{x}} = \boldsymbol{A}\boldsymbol{x}$ where

$$\boldsymbol{A} = \begin{bmatrix} 0 & k & 0 \\ 0 & 0 & 1 \\ -F_e/M_e & -F_e/M_e - K_L/M_e & -N_L/M_e \end{bmatrix}$$

$$N_L = N_e|_{\boldsymbol{x}=0} = N_{22}\rho_d - N_{23} - kM_{23} > 0$$

$$K_L = K_e|_{\boldsymbol{x}=0} = -kN_{23} < 0.$$

To make matrix $\boldsymbol{A}$ Hurwitz, the roots of following third-order polynomial should have negative real parts

$$M_e s^3 + N_L s^2 + (F_e + K_L)s + kF_e = 0 \tag{32}$$

where the Routh-Hurwitz criterion requires that $F_e + K_L > 0$ and $N_L(F_e + K_L) > kM_eF_e$ [21]. Notice that when $k = 0$, $N_L(F_e + K_L) > kM_eF_e = 0$, there always exist a small positive value $0 < k < \sigma$ to fulfill this requirement. In real application, we recommend that the magnitude of rotational speed $\dot{\theta}$ can be set under 1 degree/s, and then the parameter k of (25) can be determined accordingly.

IV. USV Prototype Design

An underactuated catamaran prototype in Fig. 4 was fabricated and used for the experimental verification of proposed positioning control method. The main features of this prototype are listed in Table I. Each hull of the prototype is a watertight cylinder with drop-shaped head, and the load capacity is 40 kg. The USV is powered by two underwater ducted thrusters on both sides. The type of the propeller is Ka3-65 and its diameter is 8 cm. The two servo motors in thrusters are equipped with the incremental encoder, and the maximum rotational speed is 3200 RPM.

To guarantee the real-time efficiency of execution, a high-performance micro PC with Intel Core i5-9500T is adopted and runs with the Robotic Operating System (ROS). This micro PC has six ports connecting to the different sensors and the lower control units of thrusters. The inertial measurement unit (IMU) is mounted in the bow to measure the linear accelerations, the Euler angles, and the corresponding angular speed at 100 Hz. The measurement errors are within $0.05\,\mathrm{m/s^2}$, 0.1^{o}, and $0.02\,\mathrm{rad/s}$ respectively. To obtain a high-frequency feedback position, a wireless ultra wide band (UWB) measurement system is used for local positioning. The UWB bases stations are placed at the offshore flat ground with a working distance of 150 m. The UWB feedback signal is 65 Hz and the measurement accuracy is under 0.05 m. If the USV is out of the UWB working area, the RTK GPS running at 5 Hz will take charge of the position

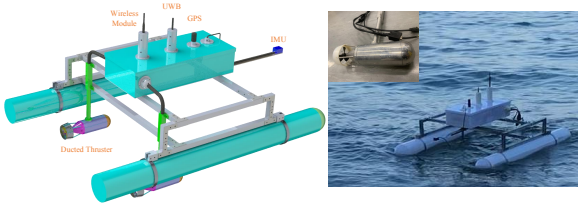

Fig. 4. The underactuated catamaran prototype.

TABLE I
MAIN FEATURES OF THE PROTOTYPE

Items	Specifications
Dimension	Long × width × draft = 1.7 m × 1.2 m × 0.09 m
Mass	40 kg
Actuators	Two thrusters driven by servo motors (50 N for each)
UWB Sensor	Distance measurement with DW1000 chip (65 Hz)
IMU Sensor	Accelerations, angular velocities, and angles (100 Hz)
RTK GPS Sensor	Ublox-F9P + 4G Network (5 Hz)
Wireless module	full-duplex connection
Onboard PC	Micro PC runs ROS
Control unit	Servo motor control and rotation feedback
Power supply	36 V 30 Ah Li-Po battery
Operating mode	Autonomous / Joystick
Ground station	Personal laptop

measurement. To establish the wireless connection between the USV and the ground station, two full-duplex wireless modules are adopted, the USV working states are fed back to the ground station at 3 Hz.

All the data of sensors are packaged and sent to the micro PC with the NMEA 0183 protocol. Then the control system in the micro PC running ROS produces the control signals to the lower control unit which can generate the desired high-frequency pulses for the servo driver. The lower control unit also has the function to record the feedback pulses of the incremental encoders and calculate the real-time rotational speeds of the motors.

V. Simulations and Experiments

The experiments were conducted at the seaside of The Hong Kong University of Science and Technology as shown in Fig. 5. According to the weather forecast, this area had winds and waves from east at that day. The inertial North-East coordinates were established with the origin set at one of UWB base stations, and the predefined desired position was set at $(38\,\mathrm{m}, 12\,\mathrm{m})$ in the inertial coordinates. Since this USV does not have accurate mathematical model, the *bis normalization* method in [8] was used to scale a supply vessel model in [17] to the dimensions of this USV. Using this scaled mathematical model in simulation, the initial position was set at $(42.5\,\mathrm{m}, 14.5\,\mathrm{m})$, the direction of external disturbances added on rigid body was set to -72^{o}, the predefined radius ρ_d to the look-ahead point $(x_o,\, y_o)$ was set to $8\,\mathrm{m}$, and the setting of the initial parameter θ was $\pi/2$ to determine the initial $(x_o,\, y_o)$. To improve the performance of positioning control, parameter k in (25) was set to 0.03 when the absolute angle deviation $|e|$ increased, and a smaller value 0.003 chosen for k if the absolute angle deviation $|e|$ decreased. All these settings in simulation are coincident with those in experiments.

A. Simulated and Experimental Results of Proposed Method

The experimental USV trajectory in horizontal plane is given in Fig. 6 with unknown external wind and waves added on the rigid body. The look-ahead point $(x_o,\, y_o)$ moves along the red dashed circle which is centered about the desired position $(38\,\mathrm{m}, 12\,\mathrm{m})$ with the $8\,\mathrm{m}$ radius. The equilibrium stable heading pointing against the direction of environmental force is obtained and shown as the red dashed straight line. The stable process of vehicle heading and angle θ updated by (25) are shown in Fig. 7(a). The results of proposed method show that the stable heading is around 108^{o} in the inertial coordinates. At the beginning, there exists the deviation between the vehicle heading and the stable heading. The none zero environmental force in sway direction makes the vehicle move along this force. With angle θ updated, the look-ahead point moves in the right way to ensure that the sway environmental force can always help to reduce the position deviation. With the updated law (25) to adjust the vehicle orientation, the results in Fig. 7(b) show that the angle offset in sway direction can converge from the initial 40^{o}. Fig. 8 and Fig. 9 show the position errors in the north and east directions. In experiments, the initial positioning error is about $4.5\,\mathrm{m}$ in north and $2.5\,\mathrm{m}$ in east, the proposed method works well within the accuracy of $0.2\,\mathrm{m}$ in north and $0.5\,\mathrm{m}$ in east. After about $150\,\mathrm{s}$, both the errors in north and east directions are within $0.5\,\mathrm{m}$. Since the equilibrium stable heading 108^{o} is quite close to the east direction, the control accuracy in east is mainly affected by the control accuracy of radius which is shown in Fig. 10. Considering that the USV works in the area with waves, the wave induced motion can induce the oscillation in positioning and affect the control accuracy of radius. Since the simulations are performed in ideal conditions, the corresponding simulated outputs do not have the oscillated responses. Overall, the motion data in simulations have a good agreement with the experiments.

B. Experimental Comparison Results and Discussion

The weather optimal positioning control (WOPC) method in [15] is modified and put into application in experiments for comparisons. The first shortage is that the original WOPC method in [15] is proposed for fully actuated marine surface vehicles, which requires high positioning accuracy for at least several days and is not the case for underactuated USVs. Secondly, it is a model-based approach via backstepping control design and derived by introducing different Lyapunov function candidates in four steps. Thus, the application of WOPC is complicated and requires accurate mathematical model and needs lots of parameters to be fine-tuned.

Compared with the WOPC approach, the look-ahead point in proposed method can be more efficiently and directly updated by angle θ. The vehicle heading outputs of WOPC in Fig. 7(a) shows that it has bigger oscillation and overshoot

Fig. 5. Experiments conducted at the seaside of HKUST.

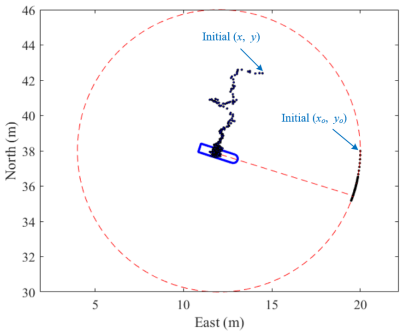

Fig. 6. The USV horizontal movement in the experiments.

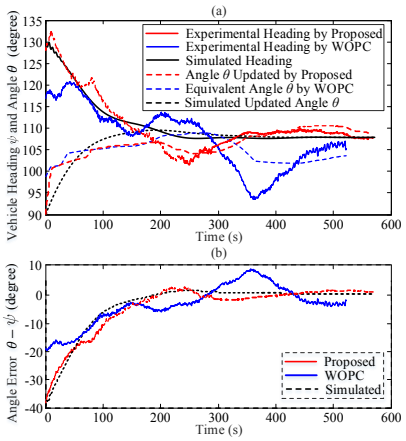

Fig. 7. The USV orientation and updated angle θ.

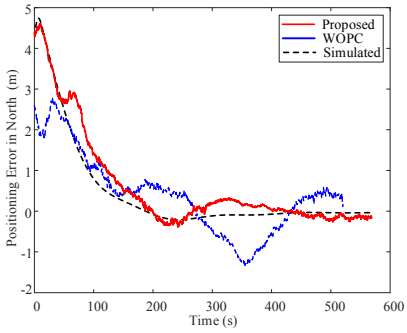

Fig. 8. USV positioning error in north direction.

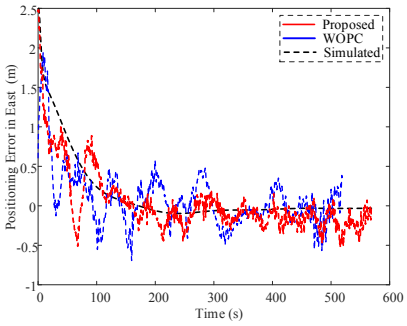

Fig. 9. USV positioning error in east direction.

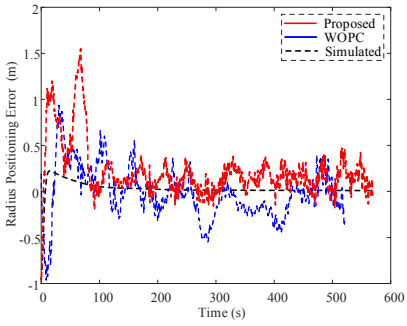

Fig. 10. USV tracking error in radius.

around the stable heading than the proposed due to the shortages mentioned above. The heading offset about 4 degree induces the weaker positioning performances in the north direction, as shown in Fig. 8.

VI. Conclusion

This paper presents and implements a vehicle-independent positioning control system for the underactuated unmanned surface vehicles to resist the external disturbances of wind, waves and currents. The implementation of this method is accomplished in three steps. The first step is to generate the yaw moment to track the orientation pointing to a look-ahead point. Next, the surge control force makes the vehicle maintain a constant distance to this look-ahead point. The last step is to derive an updated algorithm to rotate the look-ahead point around the predefined desired position such that the positioning deviation cab be minimized. To illustrate the system stability, the deviation dynamics driven by the external disturbances is derived and analyzed, which shows that the positioning deviation converges to zero with the three-step implementation. Through the experimental comparisons with existing approach, the proposed method has friendly implementation and better positioning performance.

Acknowledgment

The authors would like to thank the Key-Area Research and Development Program of Guangdong Province, China for financially supporting this work under the project no. 2018B010108004 (GDST19EG02 in HKUST).

References

[1] H. Ashrafiuon, K. R. Muske, and L. C. McNinch, "Review of nonlinear tracking and setpoint control approaches for autonomous underactuated marine vehicles," in *Proceedings of the 2010 American Control Conference*, Jun. 2010, pp. 5203–5211.

[2] S. Campbell, W. Naeem, and G. W. Irwin, "A review on improving the autonomy of unmanned surface vehicles through intelligent collision avoidance manoeuvres," *Annual Reviews in Control*, vol. 36, no. 2, pp. 267–283, 2012.
[3] Z. Liu, Y. Zhang, X. Yu, and C. Yuan, "Unmanned surface vehicles: An overview of developments and challenges," *Annual Reviews in Control*, vol. 41, pp. 71–93, 2016.
[4] W. Wang, L. A. Mateos, S. Park, P. Leoni, B. Gheneti, F. Duarte, C. Ratti, and D. Rus, "Design, modeling, and nonlinear model predictive tracking control of a novel autonomous surface vehicle," in *2018 IEEE International Conference on Robotics and Automation (ICRA)*, May 2018, pp. 6189–6196.
[5] J. G. Balchen, "Dynamic positioning using kalman filtering and optimal control theory," Amsterdam, The Netherlands, 1976, pp. 183–186.
[6] T. I. Fossen, "A survey on nonlinear ship control: from theory to practice," *IFAC Proceedings Volumes*, vol. 33, no. 21, pp. 1–16, Aug. 2000.
[7] A. J. Srensen, "A survey of dynamic positioning control systems," *Annual Reviews in Control*, vol. 35, no. 1, pp. 123–136, Apr. 2011.
[8] T. I. Fossen, *Handbook of marine craft hydrodynamics and motion control*. John Wiley & Sons, May 2011.
[9] Y. Qu, L. Cai, and H. Xu, "Curved path following for unmanned surface vehicles with heading amendment," *IEEE Transactions on Systems, Man, and Cybernetics: Systems*, 2019.
[10] K. Pettersen and O. Egeland, "Exponential stabilization of an underactuated surface vessel," in *Proceedings of 35th IEEE Conference on Decision and Control*, vol. 1, Dec. 1996, pp. 967–972 vol.1.
[11] ——, "Robust control of an underactuated surface vessel with thruster dynamics," in *Proceedings of the 1997 American Control Conference*, vol. 5, Jun. 1997, pp. 3411–3415 vol.5.
[12] K. Y. Pettersen and H. Nijmeijer, "Global practical stabilization and tracking for an underactuated ship - a combined averaging and backstepping approach," *Modeling, Identification and Control*, vol. 20, no. 4, pp. 189–199, 1999.
[13] F. Mazenc, K. Pettersen, and H. Nijmeijer, "Global uniform asymptotic stabilization of an underactuated surface vessel," *IEEE Transactions on Automatic Control*, vol. 47, no. 10, pp. 1759–1762, 2002.
[14] K. Pettersen, F. Mazenc, and H. Nijmeijer, "Global uniform asymptotic stabilization of an underactuated surface vessel: experimental results," *IEEE Transactions on Control Systems Technology*, vol. 12, no. 6, pp. 891–903, Nov. 2004.
[15] T. I. Fossen and J. P. Strand, "Nonlinear passive weather optimal positioning control (WOPC) system for ships and rigs: experimental results," *Automatica*, vol. 37, no. 5, pp. 701–715, May 2001.
[16] T. I. Fossen, S. I. Sagatun, and A. J. Sørensen, "Identification of dynamically positioned ships," *Control Engineering Practice*, vol. 4, no. 3, pp. 369–376, 1996.
[17] R. Skjetne, . N. Smogeli, and T. I. Fossen, "A nonlinear ship manoeuvering model: identification and adaptive control with experiments for a model ship," *Modeling, Identification and Control*, vol. 25, no. 1, pp. 3–27, Jan. 2004.
[18] E. Panteley and A. Loria, "On global uniform asymptotic stability of nonlinear time-varying systems in cascade," *Systems & Control Letters*, vol. 33, no. 2, pp. 131–138, 1998.
[19] A. Chaillet and A. Loría, "Uniform semiglobal practical asymptotic stability for non-autonomous cascaded systems and applications," *Automatica*, vol. 44, no. 2, pp. 337–347, 2008.
[20] H. K. Khalil, *Nonlinear systems (3rd edition)*. Prentice Hall, 2001.
[21] R. C. Dorf and R. H. Bishop, *Modern control systems*. Pearson, 2011.